This article has been accepted for publication in a future issue of this journal, but has not been fully edited. Content may change prior to final publication. Citation information: DOI 10.1109/JIOT.2018.2837891, IEEE Internet of Things Journal

Distributed Compressive Sensing Augmented Wideband Spectrum Sharing for Cognitive IoT

Xingjian Zhang, *Student Member, IEEE,* Yuan Ma, *Member, IEEE,* Haoran Qi, *Student Member, IEEE,* Yue Gao, *Senior Member, IEEE*, Zhixun Xie, Zhiqin Xie, Minxiu Zhang, Xiaodong Wang, Guangliang Wei and Zheng Li

***Abstract*—The increasing number of Internet of things (IoT) objects has been a growing challenge of the current spectrum supply. To handle this issue, the IoT devices should have cognitive capabilities to access the unoccupied portion of the wideband spectrum. However, most IoT devices are difficult to perform wideband spectrum sensing using either conventional Nyquist sampling system or sub-Nyquist sampling system since both the power-hungry sampling components and intricate sub-Nyquist sampling hardware are unrealistic in the power-constrained IoT paradigm. In this paper, we propose a blind joint sub-Nyquist sensing scheme by utilizing the surround IoT devices to jointly sample the spectrum based on the multi-coset sampling theory. Thus, only the off-the-shelf low-rate analog-to-digital converters (ADCs) on the IoT devices are required to form coset samplers and only the minimum number of coset samplers are adopted without the prior knowledge of the number of occupied channels and signal-to-noise ratios. Moreover, to further reduce the number of coset samplers and transfer part of the computational burden from the IoT devices to the core network, we adopt the data from geo-location database when applicable. The experimental results on both the simulated and real-world signals verify the theoretical results and the effectiveness of the proposed scheme. At the meanwhile, it is shown that the adaptive number of coset samplers could be adopted without causing the degradation of the detection performance and the number of coset samplers could be further reduced with the assists from geo-location database even when the obtained information is partially correct.**

***Index Terms*—Compressive Sensing, Sub-Nyquist Wideband Spectrum Sharing, Internet of Things.**

I. Introduction

The recent developments of Internet of things (IoT) has drawn world-wide attention of both academia and industry with the vision of extending Internet connectivity to a vast number of "things" in our physical world [1]–[4]. With turning IoT paradigm into a reality, the amount of IoT devices is expected to grow in large numbers, which leads to difficulty in allocating sufficient spectrum bands to these devices. Additionally, transmission performance degeneration will be caused due to the overcrowding in the unlicensed industrial, scientific and medical (ISM) bands [5]. On the other hand, not every channel in every portion of the spectrum is fully utilized all the time even for the 'busy' spectrum below 6 GHz in the urban areas, as shown in Fig. 1. This observation has encouraged the standardization bodies such as Federal Communications Commission (FCC) in U.S. and Office of Communications (Ofcom) in U.K. to release the underutilized licensed bands such as TV white space (TVWS) [6] and 3.5GHz shared spectrum [7] for temporary secondary access through the use of dynamic wideband spectrum sharing. For example, It has shown that over 50% of locations in the UK are likely to have more than 150 MHz of vacant TV spectrum and that even 90% of locations might have around 100 MHz of spectrum available [6]. Moreover, the superior penetration propagation characteristic over Ultra High Frequency (UHF) spectrum enables TVWS to have longer communication distance and better penetration through obstacles [8], which makes TVWS be an ideal candidate for the long-range wide-area IoT network, especially for the smart agriculture in rural area. Therefore, it is the vision that smart IoT devices should have cognitive capabilities to enable spectrum sharing over wideband spectrum [9]–[11]. With cognitive capabilities, interference among the IoT devices can be alle viated by seeking for the vacant channels through dynamic spectrum access.

The precondition for implementing the dynamic spectrum access in IoT paradigm over TVWS or other shared spectrum is the real-time observation of spectrum occupancy status. One of the current operational mechanism to attain this information is using the geo-location databases. However, it only protects registered primary systems and those databases are only available in certain locations and spectrum, e.g., TVWS in U.K. and U.S. [12]. For the concern of limited access to database and the database update speed, spectrum sensing, as one of the vital important technologies in cognitive radio (CR), was proposed to efficiently explore the underutilized spectrum [13].

However, it is unrealistic to directly acquiring the wideband signals by conventional Nyquist sampling scheme, especially in the energy-constrained IoT devices, since that requires high sampling rates (double or more than the bandwidth of the signal in frequency domain) and high power consumption in the analog-to-digital converter (ADC). In [14], [15], sequential

This work was supported by the Research and Innovation Bridges Cooperation Program between UK and China by the Ministry of Science and Technology in China with grant 2016YFE0124200, Innovate UK, Biotechnology and Biological Sciences Research Council (BBSRC), and Engineering and Physical Sciences Research Council (EPSRC) in the UK.

Xingjian Zhang, Yuan Ma, Haoran Qi and Yue Gao are with the School of Electronic Engineering and Computer Science, Queen Mary University of London, London E1 4NS, U.K. (emails:{xingjian.zhang, y.ma, h.qi}@qmul.ac.uk, yue.gao@ieee.org).

Zhixun Xie, Zhiqin Xie, and Minxiu Zhang are with Guangxi Veterinary Research Institute, Nanning, Guangxi 530001, China (emails: xiezhixun@126.com, {647968631, 285254780}@qq.com).

Xiaodong Wang, Guangliang Wei, and Zheng Li are with Guangxi TalentCloud Information Technology Co., Ltd, Nanning, Guangxi 530000, China (emails:{wxd, wgl, lz}@tcloudit.com).

This article has been accepted for publication in a future issue of this journal, but has not been fully edited. Content may change prior to final publication. Citation information: DOI 10.1109/JIOT.2018.2837891, IEEE Internet of Things Journal

sensing approaches were proposed to individually sense the channels by using the tunable narrowband bandpass filter with low-rate ADC. Due to the sequential nature of those schemes, the large sensing latency would be introduced, which may lead to missed opportunities or interferences [16]. Therefore, compressive sensing (CS) [17], [18] was applied to to realize wideband spectrum sensing without the high rate signal sampling and processing. It enables the fast and accurate spectrum detection with sub-Nyquist sampling rates by exploiting the sparse nature of the underutilized wideband spectrum in practice [19], [20]. However, the specialized sampling schemes for CS are difficult to be implemented in most of compact IoT devices with limited energy supply and cost constraints. For example, the random demodulation sampling [21] which employs the high rate pseudorandom sequence to modulate the input signal, and the conventional multi-coset sampling [22]–[24] which have to assemble numerous ADCs into a single sensing equipment due to the unknown number of occupied channels in practice.

Therefore, the wideband spectrum sensing scheme without employing either high-rate ADCs or specialized sampling schemes is urgently needed for low-power IoT scenario. On the other hand, as the rapid growth of low-power IoT market, large number of IoT devices would be deployed closely in order to achieve multiple environment sensing and machine control functions, which are equipped with commercial low-rate ADCs for data transmission [25]. Motivated by the above challenges, the contribution of this paper is threefold.

Firstly, we propose a distributed sub-Nyquist sampling scheme by utilizing adjacent IoT devices which have cognitive capabilities with wide-range radio frequency (RF) front-end, to jointly sample the spectrum based on the multi-coset sampling theory. It means that only the off-the-shelf low-rate ADC on each IoT device is required for sampling and formed as the coset sampler. Secondly, we consider the situation in which the number of occupied channels is unknown. As the multi-coset sampling theory indicates that the number of cosets should be at least more than two times of the number of occupied channels [22], in the conventional multi-coset sampling scheme [22]–[24], the prior knowledge of occupied channel number is required to adopt the minimum number of cosets, which is difficult to know in practice. Furthermore, even the number of occupied channels is known, the least number of coset to achieve the same detection performance is varying under different signal-to-noise ratios (SNRs) [23]. Therefore, the aforementioned schemes tend to further increase the amount of cosets in order to keep stable detection performance. In the proposed scheme, only the minimum number of coset samplers are adopted without the prior knowledge of occupied channel number by gradually increasing the number of involved coset samplers and indirectly estimating the reconstruction errors until the spectrum recovery is satisfactory. Thirdly, we propose to incorporate the channel occupancy information from geo-location database when it is applicable. In [26], a database-assisted CS algorithm employs the channel historical power information from geo-location database to reduce the iterations of weights updating in the iteratively reweighted least square (IRLS) algorithm. However, the dynamic change of channel power information from geo-location database could severely degrade the reconstruction accuracy, i.e., newly added PUs and the errors in the prior information from geo-location database. Therefore, we proposed a hybrid reconstruction scheme with the awareness that the prior information from geo-location is not perfectly reliable. Moreover, the proposed can track the changes of spectrum occupancy state in real-time, i.e., newly added users. With the assists from geo-location database, part of the complexity of local wideband sensing is transferred to the core network, thus further decreasing the processing complexity and energy consumption required on the IoT devices.

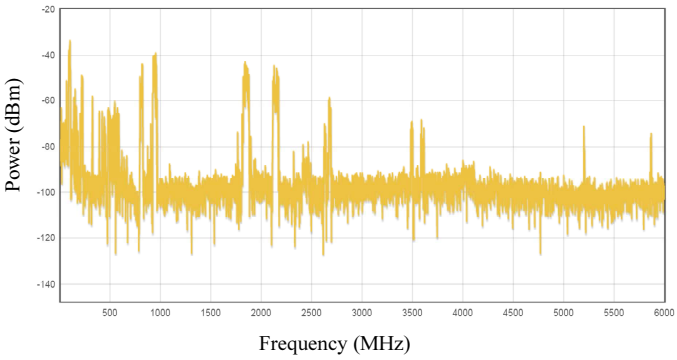

Fig. 1. The real-time spectrum occupancy recorded at Queen Mary University of London (51.523021°N 0.041592°W). The figure shows that the spectrum is sparsely occupied below 6 GHz.

The rest of this paper is organized as follows: Section II describes the preliminary system and signal model. In Section III, the proposed blind joint sub-Nyquist sensing scheme is introduced. Section IV introduces the joint iterative reweighted sparse recovery incorporated with geo-location database. Section V analyzes and validates the proposed algorithms over simulated and real-world TVWS signals. Conclusions are drawn in Section VI.

II. Preliminary System Model and Problem Formulation

A. System Model

In this paper, we consider that the observed wideband spectrum signal $x(t)$ is a continuous-time signal whose total bandwidth is denoted as W Hz, such that

$$x(t) = \sum_{i=1}^{N_{\text{sig}}} [s_i(t) + n_i(t)], \tag{1}$$

where N_{sig} is the number of transmission signals from primary users (PUs). $s_i(t)$ and $n_i(t)$ refers to the i-th signal and additive white Gaussian noise (AWGN) in the corresponding band respectively. In the conventional Nyquist sampling system, the sampling rate is adopted as $f_N \geq 2W$ over the observation time T_o to generate the uniform samples $x[\frac{n}{f_N}]$.

This article has been accepted for publication in a future issue of this journal, but has not been fully edited. Content may change prior to final publication. Citation information: DOI 10.1109/JIOT.2018.2837891, IEEE Internet of Things Journal

The corresponding discrete Fourier transform (DFT) of the signal $x[\frac{n}{f_N}]$ could be obtained as

$$X[k] = \sum_{n=0}^{N-1} x\left[\frac{n}{f_N}\right] e^{-2\sqrt{-1}\pi kn/N}, \quad k = 0, 1, \ldots, N-1, \tag{2}$$

where $N = f_N \cdot T_o$ and $X[k]$ typically bears a near sparse property due to the underutilization of wideband spectrum as shown in Fig. 1. Without loss of generality, the wideband spectrum is evenly segmented into H channels. Since the probabilities that PUs present in any channel are assumed to be unknown, we model the multiband sensing on each channel as a binary hypothesis test [27]. The general compressive spectrum sensing framework utilized in the proposed scheme is illustrated in Fig. 2. The aim of compressive spectrum sensing is to reconstruct signal $x[\frac{n}{f_N}]$ or its spectrum $X[k]$ from the sub-Nyquist samples and then perform the spectrum sensing techniques, e.g., energy detection and feature detection, on the reconstructed signal in order to decide the occupancy status. Compared with other conventional spectrum detection technologies [28], the energy detection does not require any prior knowledge of the PUs, i.e., modulation type, with lower implementation and computational complexity [29], therefore, we adopt the energy detection method [30] in this paper.

In the context of wideband spectrum sensing in shared spectrum, some of the frequency bands are heavily used by the primary users such as local radio stations, local TV stations, etc., so the related information at the geo-location database will be stable due to TV broadcasting arrangement in the long run (e.g., years). Therefore, although the side-information from geo-location database is possibly with some errors due to the dynamic changes of the spectrum state, such information can be incorporated at the sensing terminals to reduce the sensing costs.

B. Problem Formulation

According to the general CS-based spectrum sensing framework shown in Fig. 2, we know that the spectrum recovery performance would have direct impact on the sensing results. For the compressive multi-coset sampling theory, the reconstruction performance mainly depends on three factors: the number of cosets, the reconstruction algorithm and the occupancy ratio, i.e., bandwidth of transmission signals/total bandwidth. As the occupancy ratio is determined by transmission activities within the desired wideband spectrum. In this paper, we focus on discussing how to choose the minimum number of cosets samplers without the prior knowledge of the occupied channel number and how to optimize the reconstruction stage in terms of number of required measurements and computational burden with the coexistence of dynamic incumbent systems over TVWS.

The compressive measurement acquisition can be expressed by the following analytical model:

$$\boldsymbol{y} = \boldsymbol{\Phi}\boldsymbol{x} + \boldsymbol{\xi} \quad \text{subject to } ||\boldsymbol{x}||_0 \leq s, \tag{3}$$

where $\boldsymbol{\Phi} \in \mathbb{R}^{M \times N}$ is the measurement matrix to collect the compressive samples $\boldsymbol{y} \in \mathbb{R}^M$ from the original signal $\boldsymbol{x}$.

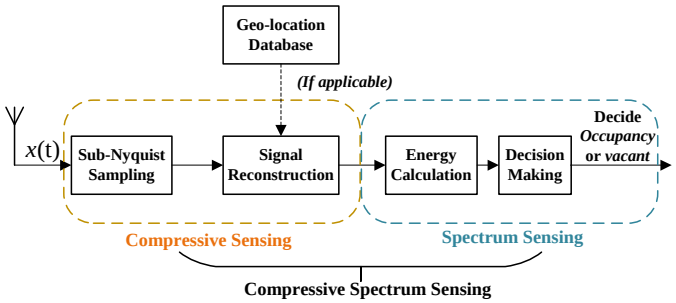

Fig. 2. Block diagram of compressive spectrum sensing framework.

$M \in \mathbb{Z}$ (with $s < M < N$) refers to the dimension of $\boldsymbol{y}$, and $||\cdot||_0$ represents the number of nonzero elements in the vector, which is also treated as the measure of sparsity. Parameter $\boldsymbol{\xi} \in \mathbb{R}^M$ is the noise perturbation, whose magnitude is constrained by an upper bound η, i.e., $||\boldsymbol{\xi}||_2 < \eta$.

Under certain assumptions including the restricted isometry property (RIP) on $\boldsymbol{\Phi}$ and the signal sparsity bound [17], robust signal reconstruction with respect to the above linear system can be formulated as the following unconstrained minimization problem:

$$\boldsymbol{x}^* := \arg\min_{\boldsymbol{x} \in \mathbb{R}^N} \frac{1}{2}||\boldsymbol{\Phi}\boldsymbol{x} - \boldsymbol{y}||_2^2 + \lambda||\boldsymbol{x}||_0, \tag{4}$$

where $\boldsymbol{x}^*$ is the reconstructed signal and constant parameter $\lambda > 0$ is introduced to balance the objective of minimizing the reconstruction error $||\boldsymbol{x} - \boldsymbol{x}^*||_2^2$ and the solution sparsity $||\boldsymbol{x}||_0$ according to the Lagrange multiplier theorem. However, problem (4) is NP-hard due to the l_0-norm minimization of $\boldsymbol{x}$. It was shown in [17] that the result of l_0-norm minimization can be equivalent to the solution obtained by the l_1-norm minimization which can be solved in polynomial time. Therefore, (4) can be approximated as

$$\boldsymbol{x}^* := \arg\min_{\boldsymbol{x} \in \mathbb{R}^N} \frac{1}{2}||\boldsymbol{\Phi}\boldsymbol{x} - \boldsymbol{y}||_2^2 + \lambda||\boldsymbol{x}||_1. \tag{5}$$

Recent works [31] show that additional prior knowledge on the original signal can be utilized to enhance the reconstruction capabilities of CS algorithms. For example, the signal reconstruction stage could adapt to the incomplete or complete prior information on the support of original signal in sparse domain, e.g., frequency spectrum, which aims to obtain a result that explains the samples, whose support contains the smallest number of new additions to the known support $\mathcal{T}$ and subject to the target sparsity, so the solution is given by

$$\boldsymbol{x}^* := \arg\min_{\boldsymbol{x} \in \mathbb{R}^N} \frac{1}{2}||\boldsymbol{\Phi}(\boldsymbol{x})_{\mathcal{T}^c} - \boldsymbol{y}||_2^2 + \lambda||(\boldsymbol{x})_{\mathcal{T}^c}||_1. \tag{6}$$

Suppose that the support set of $\boldsymbol{x}$ is denoted as $\mathcal{S} = \text{supp}(\boldsymbol{x})$, where the known part of the support set is $\mathcal{T}$, the unknown support set is $\mathcal{U}$ and the error in the known part set is $\mathcal{U}_e := \mathcal{T} \backslash \mathcal{S}$. The size of these sets are denoted as $s := |\mathcal{S}|$, $u := |\mathcal{U}|$ and $e := |\mathcal{U}_e|$, so that $s = t + u - e$. The theoretical lower bound for exact reconstruction based on the l_0-norm minimization can be expressed with the restricted orthogonality constant δ as [32]

$$\delta_{t+2u} < 1, \tag{7}$$

This article has been accepted for publication in a future issue of this journal, but has not been fully edited. Content may change prior to final publication. Citation information: DOI 10.1109/JIOT.2018.2837891, IEEE Internet of Things Journal

which is much weaker than that of the original sparse recovery $\delta_{2s} < 1$ [31] as the restricted orthogonality constant δ is nondecreasing, and $s \gg u$; $s \gg e$. Sufficient condition for exact reconstruction in terms of δ measures the theoretical minimum number of samples needed. Therefore incorporating the prior known part of the signal support can reduce the number of samples to guarantee the successful reconstruction, so that the sampling rate and computational burden will be further reduced for the power-constrained IoT devices.

The notation used is summarized as follows. The superscripts $(\cdot)^T$, $(\cdot)^H$ denote transpose, Hermitian transpose respectively. $\boldsymbol{A}_{i,j}$ is the (i,j)-th entry of the matrix $\boldsymbol{A}$. $\boldsymbol{A}_{(i)}$ is the i-th column of the matrix $\boldsymbol{A}$. $\boldsymbol{A}_{[i]}$ is the i-th row of the matrix $\boldsymbol{A}$. $\boldsymbol{A}_{\mathcal{T}}$ denotes the sub-matrix containing the columns of $\boldsymbol{A}$ with indices from $\mathcal{T}$. The notation $\mathcal{T}^c$ denotes the complement of the set $\mathcal{T}$. $\mathcal{T}_1 \backslash \mathcal{T}_2 = \mathcal{T}_1 \cap \mathcal{T}_2^c$ denotes the set difference. And $|\mathcal{T}|$ denotes the size of set $\mathcal{T}$. vec$(\cdot)$ operator refers as vec$(\boldsymbol{A}) \triangleq [\boldsymbol{A}_{(1)}^T, \boldsymbol{A}_{(2)}^T, \ldots,]^T$ and supp$(\boldsymbol{x})$ denotes the support set of $\boldsymbol{x}$.

III. The Proposed Blind Joint Sub-Nyquist Sensing Scheme

In this section, the proposed blind joint sub-Nyquist sensing scheme is presented, which utilizes adjacent IoT devices to jointly sense the wideband spectrum. Compared with the conventional multi-coset sampling scheme, the adaptive number of cosets samplers are adopted without the prior knowledge of the occupied channel number.

As shown in Fig. 3, the joint sub-Nyquist sensing system is realized by utilizing multiple IoT devices which are served as low-rate coset samplers, and the edge computing unit which could be either the IoT device or independent computing unit if the IoT device with sufficient power supply and computing capability is not available in surrounding area. The power-constrained IoT devices could benefit from transferring the computing task to the edge computing unit, especially for those IoT devices with sensing capability but sufficient computing resource. Given the number of channels H and corresponding Nyquist sampling rate $f_N = 1/T_N \geq 2W$, each of the coset samplers takes uniform samples by a significantly decreased sampling rate $f_s = \frac{1}{HT_N} = f_N/H$ with a time offset of $\{c_i T_N\},\ i = 1, ..., p$, where $p < H$ is the number of coset samplers and the set $\mathcal{C} = \{c_i\}_{i=1}^p$ consists of p distinct integers randomly selected from $[0, H-1]$. Thus the average compressive ratio could be given as $\alpha = (f_N/H)T_N \cdot p/(f_N \cdot T_N) = p/H$. For the i-th coset sampler, the uniform sampling sequence is defined as

$$x_{c_i}[n] = \begin{cases} x(nT_N), & n = mH + c_i,\ m \in \mathbb{Z} \\ 0, & \text{otherwise.} \end{cases} \tag{8}$$

Furthermore, by applying Fourier transform to $x_{c_i}[n]$, the relationship between its spectrum $X_{c_i}(e^{2\sqrt{-1}\pi k T_N})$ and the unknown Fourier spectrum $X(k)$ of $x(t)$ is presented as [33]

$$X_{c_i}(e^{2\sqrt{-1}\pi k T_N}) = \frac{1}{HT_N} \sum_{h=0}^{H-1} X_h(k) e^{\sqrt{-1}\frac{2\pi}{H} c_i h},\ \forall k \in [0, W], \tag{9}$$

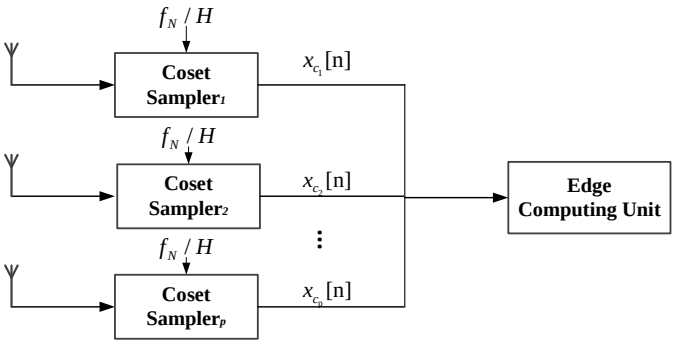

Fig. 3. Block diagram of the proposed joint sub-Nyquist sensing system.

for every $1 \leq i \leq p$, where $X_h(k) = X(k + \frac{h}{HT_N})$ corresponds to the pieces of the original spectrum $X(k)$ in the h-th channel, which is shifted to the left by $\frac{h}{HT_N}$ units. Therefore, (9) could be simplified into the matrix form as

$$\boldsymbol{Y}(k) = \boldsymbol{A}\boldsymbol{X}(k),\ \forall k \in [0, W], \tag{10}$$

where $\boldsymbol{Y}(k) \in \mathbb{C}^{p \times L}$ is a matrix whose i-th row is $X_{c_i}(e^{2\sqrt{-1}\pi k T_N})$, $\boldsymbol{X}(k) = [X_0(k), X_1(k), ..., X_{H-1}(k)]^T$ is the unknown spectrum vectors of $x(t)$ in the H channels, and $\boldsymbol{A} \in \mathbb{C}^{p \times H}$ is a matrix with (i,j)-th element given by $\boldsymbol{A}_{i,j} = \frac{1}{HT_N} e^{\sqrt{-1}\frac{2\pi}{H} c_i (j-1)}$.

The multi-coset sampling theory indicates that the number of cosets p should be at least more than two times of the number of occupied channels [22]. Therefore, in the conventional multi-coset sampling scheme [22], [23], the number of occupied channels κ is assumed as the prior knowledge to decide the number of coset p needed in integrated sampling hardware. However, as the number of occupied channels is unknown in practice, p could be set unnecessary large when it is determined by κ. Moreover, even if the exact number of occupied channels is known or estimated, the least number of cosets to achieve the same detection performance are still varying under different SNRs [23]. Therefore, fixing the number of coset when produce the sampling hardware could cause either performance degeneration or the waste of sampling resources.

In the proposed scheme, only the minimum coset samplers are adopted without the prior knowledge of the number of occupied channels or its upper bound value κ. Specifically, through repeating the procedure of signal acquisition by gradually increasing the number of involved coset samplers and performing signal reconstruction, we could obtain a sequence of reconstructed signal, i.e., $\hat{\boldsymbol{x}}_{\boldsymbol{1}}, \hat{\boldsymbol{x}}_{\boldsymbol{2}}, \cdots, \hat{\boldsymbol{x}}_{\boldsymbol{p}}$, where $\hat{\boldsymbol{x}} = \text{vec}(\hat{\boldsymbol{X}}(k))$. After each time of signal reconstruction, the proposed scheme should decide whether the reconstruction of the original signal is accurate enough or not. If the reconstructed signal does not satisfy certain accuracy requirement of spectral detection, the scheme should require more coset samplers until the accuracy of the signal reconstruction is good enough. However, the actual reconstruction error $e = ||\boldsymbol{x} - \hat{\boldsymbol{x}}||_2^2$ is inaccessible since the original signal $\boldsymbol{x} = \text{vec}(\boldsymbol{X}(k))$ is unknown. In this paper, we propose to estimate the reconstruction error e indirectly and set stopping criterion.

This article has been accepted for publication in a future issue of this journal, but has not been fully edited. Content may change prior to final publication. Citation information: DOI 10.1109/JIOT.2018.2837891, IEEE Internet of Things Journal

Before proposing the scheme to approximate reconstruction error, we give the vectorization of (10) in the following lemma.

Lemma 1. *Given the matrix form $\boldsymbol{Y}(k) = \boldsymbol{A}\boldsymbol{X}(k)$, we could obtain the vector form as vec$(\boldsymbol{Y}(k)) = \boldsymbol{\Phi}vec(\boldsymbol{X}(k))$, where the matrix $\boldsymbol{\Phi} = \boldsymbol{I_L} \otimes \boldsymbol{A}$ and the operator $\otimes$ represents the Kronecker product.*

Proof. Let $\boldsymbol{X}(k) = [\boldsymbol{X}_{(1)}(k), \boldsymbol{X}_{(2)}(k), \cdots, \boldsymbol{X}_{(L)}(k)]$ and $\boldsymbol{u_1}, \boldsymbol{u_2}, \cdots, \boldsymbol{u_L}$ denote the unit vectors. We could obtain

$$\begin{aligned}
\text{vec}(\boldsymbol{Y}(k)) &= \text{vec}(\boldsymbol{A}\boldsymbol{X}(k)) = \text{vec}(\boldsymbol{A}\boldsymbol{X}(k)\boldsymbol{I_L}) \\
&= \text{vec}\Big(\sum_{i=1}^{L} \boldsymbol{A}\boldsymbol{X_i}(k)\boldsymbol{u_i}^T\boldsymbol{I_L}\Big) \\
&= \sum_{i=1}^{L} \text{vec}\big((\boldsymbol{A}\boldsymbol{X_i}(k))(\boldsymbol{I_L}\boldsymbol{u_i})^T\big) \\
&= \sum_{i=1}^{L} \big(\boldsymbol{I_L}\boldsymbol{u_i} \otimes \boldsymbol{A}\boldsymbol{X_i}(k)\big) \\
&= (\boldsymbol{I_L} \otimes \boldsymbol{A}) \sum_{i=1}^{L} \big(\boldsymbol{u_i} \otimes \boldsymbol{X_i}(k)\big) \\
&= (\boldsymbol{I_L} \otimes \boldsymbol{A}) \sum_{i=1}^{L} \text{vec}\big(\boldsymbol{X_i}(k)\boldsymbol{u_i}^T\big) = \boldsymbol{\Phi}\text{vec}(\boldsymbol{X}(k))
\end{aligned} \tag{11}$$

Thus vec$(\boldsymbol{Y}(k)) = $ vec$(\boldsymbol{A}\boldsymbol{X}(k)) = \boldsymbol{\Phi}vec(\boldsymbol{X}(k))$ is obtained. □

In the following of this section, we denote vec$(\boldsymbol{Y}(k))$ as $\boldsymbol{y}$. Specifically, the samples vector $\boldsymbol{y}$ in each step is divided into two vectors $\boldsymbol{y_r}$ ($\boldsymbol{y_r} \in \mathbb{R}^{r\times 1}$) and $\boldsymbol{y_v}$ ($\boldsymbol{y_v} \in \mathbb{R}^{v\times 1}$). According to Lemma 1, these two vectors therefore can be expressed as $\boldsymbol{y_r} = \boldsymbol{\Phi_r}\boldsymbol{x}$ and $\boldsymbol{y_v} = \boldsymbol{\Phi_v}\boldsymbol{x}$ respectively, where $\boldsymbol{\Phi_r}$ is a $r \times HL$ matrix and $\boldsymbol{\Phi_v}$ is a $v \times HL$ matrix. Parameter r represents the number of samples in $\boldsymbol{y_r}$ for signal recovery and v is the number is set to guarantee the sufficient accuracy of reconstruction error estimation as illustrated later.

As mentioned before, the exact reconstruction error $e = ||\boldsymbol{x} - \hat{\boldsymbol{x}}||_2^2$ could not be obtained to determine how accuracy the reconstructed signal is. Therefore, we propose to estimate the actual reconstruction error e indirectly by using the verification vector $\boldsymbol{y_v}$ and the proposed stopping criterion is defined as

$$S_p = ||\boldsymbol{\Phi_v}\hat{\boldsymbol{x}} - \boldsymbol{y_v}||_2^2. \tag{12}$$

The Johnson-Lindenstrauss Lemma presented in [34] asserts that a high-dimensional space can be projected into a low-dimensional one whose dimension is equal or larger than $O(\zeta^{-2}\log HL)$ so that all distances are preserved up to a multiplicative factor between $1-\zeta$ and $1+\zeta$ with the factor $\zeta \in [0, \leq 1/2]$. To demonstrate the rigorous relationship between the actual reconstruction error e and the proposed stopping parameter S_p, we prove the point that the actual reconstruction error $e = ||\boldsymbol{x} - \hat{\boldsymbol{x}}||_2^2$ could be approximated by S_p within the boundary factor of $1 \pm \zeta$ in Theorem 2. Therefore, in order to terminate the signal acquisition process, i.e., determine whether the number of coset samplers are sufficient or not, one can compare the proposed stopping parameter S_p with a predefined threshold which could be determined according to the certain reconstruction accuracy requirement.

Theorem 2. *Given $\zeta \in (0, 1/2]$, and $\gamma \in (0,1)$ and $v \leq C\zeta^{-2}log(1/2\gamma)$, we have*

$$\frac{S_p}{(1+\zeta)} \leq e \leq \frac{S_p}{(1-\zeta)} \tag{13}$$

with confidence $1-\gamma$, where the parameter C depends on the concentration property of random variables in measurement matrix $\boldsymbol{\Phi_{\Delta M}}$ [34]. $\hat{e}$ and e are defined as before.

Proof. With the aid of Johnson-Lindenstrauss Lemma, if the number of row v in $\boldsymbol{\Phi_v}$ is equal or larger than $C\zeta^{-2}\log(1/2\gamma)$, we have

$$(1-\zeta)||\boldsymbol{x} - \hat{\boldsymbol{x}}||_2^2 \leq ||\boldsymbol{\Phi_v}(\boldsymbol{x} - \hat{\boldsymbol{x}})||_2^2 \leq (1+\zeta)||\boldsymbol{x} - \hat{\boldsymbol{x}}||_2^2 \tag{14}$$

with confidence $1-\gamma$, where $\zeta \in (0, 1/2]$ and $\gamma \in (0,1)$. As matrix $\boldsymbol{\Phi_v}$ could be seen as a linear projection from $\mathbb{R}^{HL}$ to $\mathbb{R}^v$, we can get

$$\begin{aligned}
(1-\zeta)||\boldsymbol{x} - \hat{\boldsymbol{x}}||_2^2 &\leq ||\boldsymbol{\Phi_v}\hat{\boldsymbol{x}} - \boldsymbol{y_v}||_2^2 \\
&\leq (1+\zeta)||\boldsymbol{x} - \hat{\boldsymbol{x}}||_2^2.
\end{aligned} \tag{15}$$

To obtain the observation that $e = ||\boldsymbol{x} - \hat{\boldsymbol{x}}||_2^2$ could be bounded and estimated by $S_p = ||\boldsymbol{\Phi_v}\hat{\boldsymbol{x}} - \boldsymbol{y_v}||_2^2$, we change the (15) to another form (16) and simplify it to (17):

$$\begin{aligned}
\frac{1}{(1+\zeta)}||\boldsymbol{\Phi_v}\hat{\boldsymbol{x}} - \boldsymbol{y_v}||_2^2 &\leq ||\boldsymbol{x} - \hat{\boldsymbol{x}}||_2^2 \\
&\leq \frac{1}{(1-\zeta)}||\boldsymbol{\Phi_v}\hat{\boldsymbol{x}} - \boldsymbol{y_v}||_2^2,
\end{aligned} \tag{16}$$

$$\frac{S_p}{(1+\zeta)} \leq e \leq \frac{S_p}{(1-\zeta)}. \tag{17}$$

□

Therefore, when the row number v in $\boldsymbol{\Phi_v}$ is equal or larger than $C\zeta^{-2}\log(1/2\gamma)$, the distance between S_p and e could be bounded up to a multiplicative factor between $1-\zeta$ and $1+\zeta$ with the confidence $1-\gamma$.

To further reduce the computational complexity of the signal reconstruction of (10), we compute the covariance matrix of the sample sequences as [35]

$$\boldsymbol{R} = \mathbb{E}[\boldsymbol{Y}(k)\boldsymbol{Y}^H(k)] = \boldsymbol{A}\boldsymbol{R}_X\boldsymbol{A}^H, \tag{18}$$

where $\boldsymbol{R}_X = \mathbb{E}[\boldsymbol{X}(k)\boldsymbol{X}^H(k)]$ is the $H \times H$ primary signal correlation matrix and σ_n^2 is the noise variance. According to the eigenvalue decomposition (EVD) method [23], the covariance matrix $\boldsymbol{R}$ could be decomposed as $\boldsymbol{R} = \boldsymbol{U}\boldsymbol{\Lambda}\boldsymbol{U}^H$. Utilizing eigenvalues $\boldsymbol{\Lambda}$ and the corresponding eigenvectors $\boldsymbol{U}$, the measurement matrix could be constructed as $\boldsymbol{\chi} = \boldsymbol{U}\sqrt{\boldsymbol{\Lambda}}$, and we can define the following linear system

$$\boldsymbol{\chi} = \boldsymbol{A}\boldsymbol{\nu}, \tag{19}$$

where the support of the sparest solution to (19) converges to the original spectrum in matrix form, i.e., $supp(\boldsymbol{\nu}) = supp(\boldsymbol{X}(k))$ [23]. Compared with original sub-Nyquist samples $\boldsymbol{Y}(k) \in \mathbb{C}^{p\times N}$, using $\boldsymbol{\chi} \in \mathbb{C}^{p\times p}$ for support recovery reduces the computation complexity required on the SUs.

This article has been accepted for publication in a future issue of this journal, but has not been fully edited. Content may change prior to final publication. Citation information: DOI 10.1109/JIOT.2018.2837891, IEEE Internet of Things Journal

Algorithm 1 The proposed blind joint sub-Nyquist sensing scheme

Require: Sampling rate f_s, the maximum number of available coset samplers $p_{\max}$, the stopping parameter threshold δ, $\boldsymbol{A}$.

Ensure: The reconstructed signal $\hat{\boldsymbol{x}}$

while $p = 0, \cdots, p_{\max}$ **do**
  Sampling the wideband signal using f_s with p coset samplers so as to obtain the compressive measurement matrix $\boldsymbol{Y}(k)$ and the corresponding covariance matrix $\boldsymbol{R}$.
  Reconstruct the support and spectral from $\boldsymbol{R}$ by utilizing SOMP algorithm according to (19), leading to a spectral reconstruction $\hat{\boldsymbol{x}}_{\boldsymbol{p}}$.
  Calculate the stopping parameter

$$S_p = ||\boldsymbol{\Phi}_{\boldsymbol{v}}\hat{\boldsymbol{x}} - \boldsymbol{y}_{\boldsymbol{v}}||_2^2$$

  if S_p smaller than predefined threshold is true
    Terminate the signal acquisition process.
  else
    $p = p + 1$
  end if
end while

After the support recovery, the exact signal reconstruction could be achieved by the reconstruction algorithm. In CS, the original signal could be recovered from sub-Nyquist samples by solving the l_1-norm minimization. Since the reconstruction of the unknown matrix $\boldsymbol{\nu}$ with jointly sparse columns in (19) is referred to as the joint sparse problem [36], we extend greedy-type algorithm such as simultaneous orthogonal matching pursuit (SOMP) [37] to solve this joint sparse problem, because of its lower complexity compared with the l_1-norm minimization [38]. Besides, the related exact recovery criterion for the conventional orthogonal matching pursuit (OMP) remains valid for its extension to SOMP [39].

IV. Joint Iterative Reweighted Sparse Recovery with Geo-location Database

In this section, firstly we extend the single measurement vector (SMV) problem to the multiple measurement vectors (MMV) problem in (10), where $\boldsymbol{X}(k)$ is row-sparse, i.e., having nonzero entries in only a few rows. Then the l_ν-norm ($0 < \nu < 1$) minimization problem solving by the iteratively reweighted least square (IRLS)-type algorithm is modified to incorporate the information from geo-location database for enhancing the recovery performance with fewer measurements. Based on the white space channel information from the geo-location database, the sensor node can get a response with details of available channels in the vicinity. For simplifying the notation, $\boldsymbol{X}(k)$ and $\boldsymbol{Y}(k)$ are denoted as $\boldsymbol{X}$ and $\boldsymbol{Y}$ respectively.

Since the parameter H is set based on the number of channels in the spectrum of interest, the positions of nonzero rows in (10) is equivalent to the active channel index set $\mathcal{S}$. Therefore, the channel status information from geo-location database could be incorporated on the indices of the corresponding rows with large norm in the recovery process,

Algorithm 2 Iterative Reweighted Sparse Recovery with Prior Information

Require: matrix of p samples sequence $\boldsymbol{Y} \in \mathbb{C}^{p\times N}$, measurement matrix$\boldsymbol{A} = [\boldsymbol{a}_1, ..., \boldsymbol{a}_M] \in \mathbb{C}^{p\times M}$, information from geo-location database$\mathcal{T}$, $\hat{\kappa}$ from EFT, $\boldsymbol{W^{(0)}}$ and $\lambda(\boldsymbol{X^{(0)}})$.

Ensure: $\mathcal{S}$

for $l = 1, \cdots, l_{\max}$ **do**
  Compute
  $\boldsymbol{X}^{(l)} = \boldsymbol{W}^{(l-1)}\boldsymbol{A}^T(\boldsymbol{A}\boldsymbol{W}^{(l-1)}\boldsymbol{A}^T + \lambda(\boldsymbol{X}^{(l-1)})\boldsymbol{I})^{-1}\boldsymbol{Y}$
  if $||\Delta\boldsymbol{X}^{(l+1)}|| \leq \delta$ break;
  Update
  Weights: $w_i^{(l)} = (||\boldsymbol{X}^{(l-1)}[i]||_2)^{v-2}$
  Penalty parameter:
  $\lambda(\boldsymbol{X}^{(l)}) = \frac{1}{2}||\boldsymbol{A}\boldsymbol{X}^{(l)} - \boldsymbol{Y}||_2^2/[\varrho - \sum w_i^{(l)}(||\boldsymbol{X}_{[i]}^{(l)}||_2)^2]$
  $l = l + 1$
end for
Estimate support $\mathcal{S}$ by selecting the position of the first $\hat{\kappa}$ smallest components in $\boldsymbol{W}^{(l+1)}$
return $\mathcal{S}$=$\mathcal{S}$-1

in order to enhance the recovery performance with fewer measurements under sub-Nyquist sampling. To that end, SMV is extended to the MMV problem, where the objective is to minimize the number of rows containing nonzero entries while satisfying the measurement constraint in (10). The problem can be formulated as [36]

$$\arg\min_{\boldsymbol{X}} \frac{1}{2}||\boldsymbol{A}\boldsymbol{X} - \boldsymbol{Y}||_2^2 + \lambda||\mathcal{R}_{l_\nu}(\boldsymbol{X})||_1. \tag{20}$$

$\mathcal{R}_{l_\nu}(\boldsymbol{X})$ is a vector in $\mathbb{R}^H$ whose i-th entry is the l_ν norm of the i-th row of $\boldsymbol{X}$:

$$\mathcal{R}_{l_\nu}(\boldsymbol{X}) = [v_1, v_2, ..., v_H]^T, \tag{21}$$

where $v_i = ||\boldsymbol{X}_{[i]}||_q = (\sum_{j=1}^N |x_{i,j}|^q)^{1/q}$.

Compared with the l_1-norm minimization in (5), the l_ν-norm minimization with $0 < \nu < 1$ leads to the better sparsity approximation performance with the fewer samples since it is an intermediate problem in the sense of norm minimization between (4) and (5) [40]. Therefore the l_1-norm minimization is replaced with the l_ν-norm minimization for signal reconstruction in this section. It can be given as

$$\arg\min_{\boldsymbol{X}} \frac{1}{2}||\boldsymbol{A}\boldsymbol{X} - \boldsymbol{Y}||_2^2 + \lambda||\mathcal{R}_{l_\nu}(\boldsymbol{X})||_v^v. \tag{22}$$

where the penalty parameter $\lambda > 0$ is introduced to balance the reconstruction accuracy and the sparsity of minimization result as discussed in Section II. Since the choice of λ greatly influences the behavior of the spectrum reconstruction [41], in this work, λ is defined as a function of the target signal to optimize λ along with the signal reconstruction process, such that the problem in (22) can be transformed into the following form:

$$\arg\min_{\boldsymbol{X}} F(\boldsymbol{X}) = \frac{1}{2}||\boldsymbol{A}\boldsymbol{X} - \boldsymbol{Y}||_2^2 + \lambda(\boldsymbol{X})||\mathcal{R}_{l_\nu}(\boldsymbol{X})||_v^v. \tag{23}$$

Without losing the numerical property of (22), we define the linear function of the form: $F(\boldsymbol{X}) = \varrho\lambda(\boldsymbol{X})$ [42] to preserve

This article has been accepted for publication in a future issue of this journal, but has not been fully edited. Content may change prior to final publication. Citation information: DOI 10.1109/JIOT.2018.2837891, IEEE Internet of Things Journal

the convexity in each iteration and exhibits only a global minimizer regardless of the value of $\lambda(\boldsymbol{X})$, where ϱ is the coefficient representing the slope of the line and also controls convexity. We substitute $F(X) = \varrho\lambda(\boldsymbol{X})$ to (23) and therefore $\lambda(\boldsymbol{X})$ can be expressed as

$$\lambda(\boldsymbol{X}) = \frac{\frac{1}{2}||\boldsymbol{AX} - \boldsymbol{Y}||_2^2}{\varrho - ||\mathcal{R}_{l_\nu}(\boldsymbol{X})||_v^v} \quad 0 < \nu < 1. \tag{24}$$

However, it is general computationally hard and not guaranteed to obtain its global minimum due to the nonconvexity of the l_ν-norm minimization. It is shown in [40] that under certain assumptions such as the null space property (NSP) on measurement matrix $\boldsymbol{A}$, the solution sequence generated by the IRLS algorithm converges to the local minimum as the sparsest solution that is also the actual global l_ν-norm minimizer. With $q = 2$, each iteration of the IRLS algorithm corresponds to a convex weighted least squares subproblem that can be formulated as

$$\arg\min_{\boldsymbol{X}} \frac{1}{2}||\boldsymbol{AX} - \boldsymbol{Y}||_2^2 + \lambda(\boldsymbol{X})\sum_{i=1}^{H} w_i(||\boldsymbol{X}_{[i]}||_2)^2, \tag{25}$$

The problem in (25) will be repeatedly solved by updating the weight w_i at each iteration using the solution from previous iteration: at each iteration, w_i will be set as

$$w_i^{(l)} = (||\boldsymbol{X}_{[i]}^{(l-1)}||_2)^{v-2}. \tag{26}$$

where $w_i^{(l)},\ i = 1, ..., H$ is the value of the weighting vector to be used at the l-th iteration and $\boldsymbol{X}^{(l-1)}$ is the $(l-1)$-th iterate. After convergence, $\boldsymbol{X}^{(l-1)}$ will be sufficiently close to $\boldsymbol{X}^{(l)}$. The weighting parameter $\boldsymbol{w}^{(l)}$ are computed from the row norms of the solution obtained in the previous iteration, so the corresponding rows with smaller norm are likely to be de-emphasised as they are irrelevant in fitting the data and vice versa. In (26), as $0 < v < 1$, the weights will be chosen inversely proportional to the l_2-norm of the rows. Since it gives a large weight to the small component, it will encourage a sparse solution in the minimization problem of (25). Assuming that $\mathcal{T} \subset [0, H-1]$ is the prior knowledge of the occupied channel indices from geo-location database, its relation to the actual occupied channel set $\mathcal{S}$ can be expressed as:

$$\mathcal{S} = \mathcal{T} \cup \triangle \setminus \triangle_e, \tag{27}$$

where $\triangle := \mathcal{S} \setminus \mathcal{T}$ is newly occupied channel set, and $\triangle_e := T \setminus S$ are the newly released channel indices, i.e., the occupied channel indices recorded at geo-location database but actually released as vacant at current time.

As the i-th row in $\boldsymbol{X}$ corresponds to the piece of the original spectrum in the subchannel, the occupied channel information from geo-location database indicates the indices of the corresponding rows with large norm. Similar as (6), the objective function in (25) can therefore be changed as the l_ν minimisation over the remaining positions only, $i \notin \mathcal{T}$, i.e.,

$$\arg\min_{\boldsymbol{X}} \frac{1}{2}||\boldsymbol{AX} - \boldsymbol{Y}||_2^2 + \lambda(\boldsymbol{X})\sum_{i\notin\mathcal{T}} w_i(||\boldsymbol{X}_{[i]}||_2)^2. \tag{28}$$

By defining

$$w_i = 0, \forall i \in \mathcal{T}, \tag{29}$$

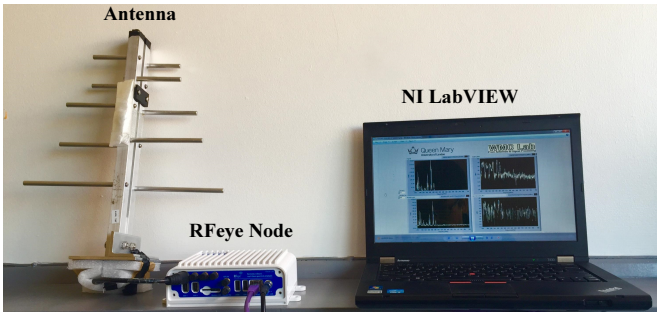

Fig. 4. Experimental setup for real-time processing and live compressive spectrum sensing testbed on TVWS [43].

the minimisation in (25) is transformed in the form of (28).

Here, in order to add the prior channel occupancy information from geo-location database, the weighing strategy in the joint sparse reconstruction is modified as

$$w_i^{(l)} = \begin{cases} \varphi(||\boldsymbol{X}_{[i]}^{(l-1)}||_2)^{v-2}, & i \in \mathcal{T} \\ (||\boldsymbol{X}_{[i]}^{(l-1)}||_2)^{v-2}, & \text{otherwise,} \end{cases} \tag{30}$$

where φ is a specified small constant. For $\varphi = 0$, the first expression in (30) reduces to 0 as required by (29).

Given an initial guess of the signal $\boldsymbol{X}^{(0)}$ (e.g., the least-squares solution), the iterative reweighting algorithm generates a sequence of iterations of as follows:

$$\begin{aligned} \boldsymbol{X}^{(l+1)} = \arg\min_{\boldsymbol{X}}\ & \frac{1}{2}||\boldsymbol{AX}^{(l)} - \boldsymbol{Y}||_2^2 + \\ & \lambda(\boldsymbol{X}^{(l)})\sum_{i\notin\mathcal{T}} w_i^{(l)}(||\boldsymbol{X}_{[i]}^{(l)}||_2)^2. \end{aligned} \tag{31}$$

The solution to (31) at the l-th iteration can be expressed as

$$\boldsymbol{X}^{(l+1)} = \boldsymbol{W}^{(l)}\boldsymbol{A}^T(\boldsymbol{A}\boldsymbol{W}^{(l)}\boldsymbol{A}^T + \lambda(\boldsymbol{X}^{(l)})\boldsymbol{I})^{-1}\boldsymbol{Y}, \tag{32}$$

where $\boldsymbol{W}^{(l)} = \text{diag}\{[1/w_1^{(l)}, ..., 1/w_H^{(l)}]\}$. The initial weight is given by

$$w_i^{(0)} = \begin{cases} \varphi, & i \in \mathcal{T} \\ 1, & \text{otherwise.} \end{cases} \tag{33}$$

The algorithm is terminated once the convergence criterion has been satisfied, i.e.,

$$||\Delta\boldsymbol{X}^{(l+1)}|| = \frac{||\boldsymbol{X}^{(l+1)} - \boldsymbol{X}^{(l)}||_2^2}{||\boldsymbol{X}^{(l)}||_2^2} \leq \delta, \tag{34}$$

where δ is a user-selected parameter. Here, based on the sparsity guess of the support dimension $\hat{\kappa}$ from exponential fitting test (EFT), the estimated active channel set is determined by selecting the position of the first $\hat{\kappa}$ smallest components in the final weight $\boldsymbol{w}$ or comparing the components with predefined threshold. The entire procedure of the proposed scheme in this section is summarised in Algorithm 2.

V. Experimental Results

In this section, we test the proposed schemes using the simulated signals as well as the real-world signals as the proof of concepts in this paper.

This article has been accepted for publication in a future issue of this journal, but has not been fully edited. Content may change prior to final publication. Citation information: DOI 10.1109/JIOT.2018.2837891, IEEE Internet of Things Journal

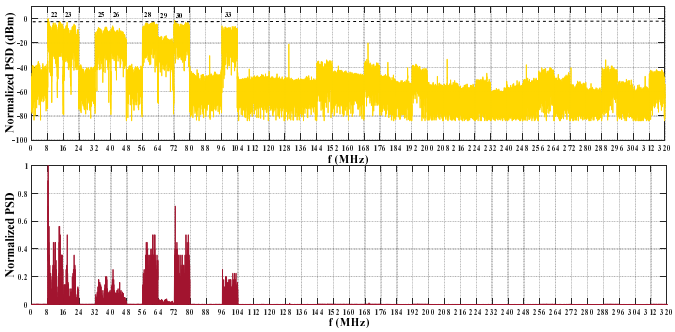

Fig. 5. Normalized power spectrum density (PSD) of the real-time TVWS signal recorded at QMUL, $\mathcal{S} = [22, 23, 25, 26, 28, 29, 30, 33]$

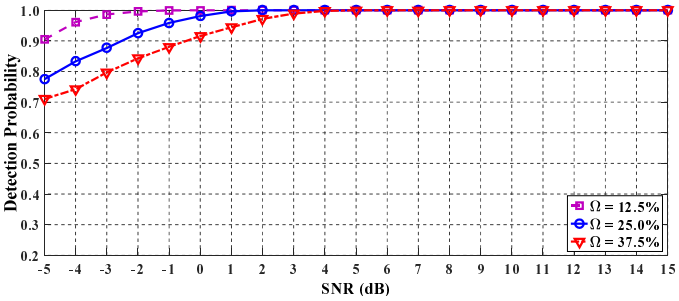

Fig. 6. Detection Probability P_d vs. SNR (dB) with $p = 20$ under different channel occupancy ratios $\Omega = 12.5\%, 25\%, 37.5\%$.

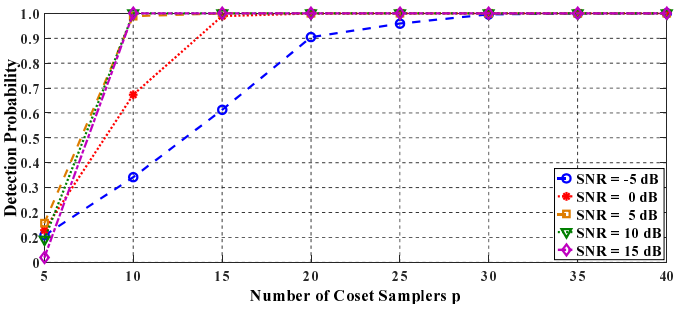

Fig. 7. Detection Probability P_d vs. number of coset samplers p with $\Omega = 12.5\%$ under different SNRs.

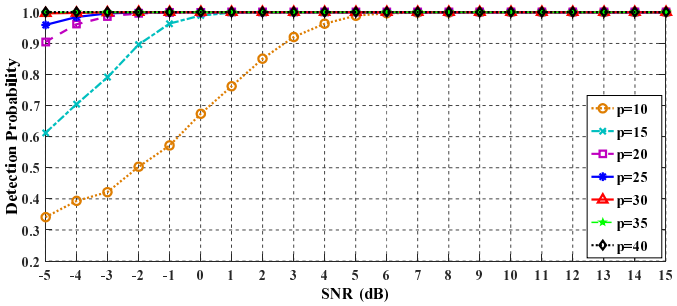

Fig. 8. Detection Probability P_d vs. SNR (dB) with $\Omega = 12.5\%$ under different number of coset samplers.

A. Experiment Setups

The simulated signals are assumed as $x(t) \in \mathcal{F} = [0, 320]$ MHz, whose DFT is denoted as $\boldsymbol{x}_0^{\text{sim}}$. To keep consistency with the real TVWS setting, the spectrum is equally divided into $L = 40$ channels with bandwidth $B_0 = 8$ MHz, which contains up to J active channels:

$$x(t) = \sum_{i=1}^{J} \sqrt{E_i B_0}\text{sinc}(B_i(t - t_i))e^{j2\pi f_i t} + n(t), \qquad (35)$$

where $\text{sinc}(x) = \sin(\pi x)/(\pi x)$, E_i, t_i and f_i represent the energy, time offset, and central frequency of the i-th channel respectively and $n(t)$ denotes the noise. The channel occupancy ratio Ω is defined as J/L. The real-world signals $\boldsymbol{x}_0^{\text{real}}$ is collected by the real-time wideband compressive spectrum sensing testbed as shown in Fig. 4. There are 40 channels (indexed as Channel 21 - Channel 60) in the recorded TVWS signal, ranging from 470 to 790 MHz and each channel contains either noise only or transmitting signal with noise. Fig. 5 shows that the normalized downconverted real-world TVWS signal in the baseband $\mathcal{F} = [0, 320]$ MHz. Strong DVB-T signal reception at channel set $\mathcal{S} = [22, 23, 25, 26, 28, 29, 30, 33]$ can be observed in the recorded spectrum. Thus the channel occupancy ratio is $\Omega = 20\%$. To quantify the detection performance, we compute the detection probability P_d, i.e., the existing of occupied channels correctly being detected as occupied, under 1000 trials.

B. Results and Analysis

1) Detection Performance versus SNR and Number of Coset samplers: Firstly, we demonstrate that channel occupancy ratio Ω affects the required minimum number of coset samplers to achieve the same detection probability P_d. It shows in Fig. 6 that the detection performance P_d against SNR from -5 dB to 20 dB with fixed number of coset samplers $p = 20$. Moreover, it is observed that P_d improves as SNR increases under different scenarios with channel occupancy ratios $\Omega = 12.5\%, 25\%, 37.5\%$, which means the minimum number of coset samplers varying with the channel occupancy ratio Ω to achieve the same detection probability P_d. However, the information of channel occupancy ratio Ω is usually unknown in practice.

To verify the theory that the better detection performance P_d always could be achieved by evolving more coset samplers, we compare P_d against different number of coset samplers p with fixed Ω and SNR. It is shown in Fig. 7 that detection performance P_d increases with the number of coset samplers but the extra coset samplers are unnecessary after the optimal detection performance is obtained by minimum number of coset samplers.

The proposed scheme could prevent the waste of sampling resources and guarantee the detection performance with sufficient number of coset samplers under different channel environments, i.e., SNRs. As demonstrated in Fig. 8, the proposed scheme therefore can be terminated according to the stopping criterion when the number of coset samplers reaches $p = 10$ if the received SNR is equal or greater than 5 dB. Besides, more coset samplers are required in the proposed scheme under the worse SNRs to achieve accurate detection performance. Therefore, it is shown that the proposed scheme is allowed to adaptively choose the number of coset samplers under different SNRs.

This article has been accepted for publication in a future issue of this journal, but has not been fully edited. Content may change prior to final publication. Citation information: DOI 10.1109/JIOT.2018.2837891, IEEE Internet of Things Journal

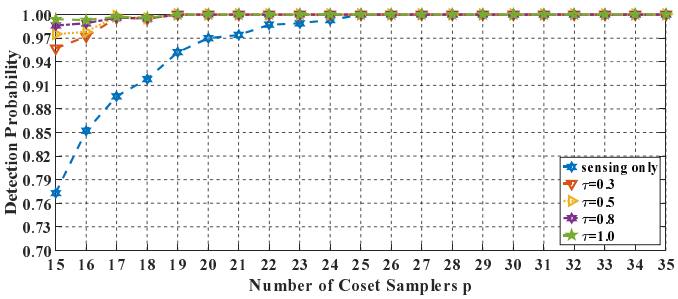

Fig. 9. Detection Probability P_d vs. number of coset samplers p under different ratio of known part $\tau = 0.3, 0.5, 0.8, 1.0$ and sensing only.

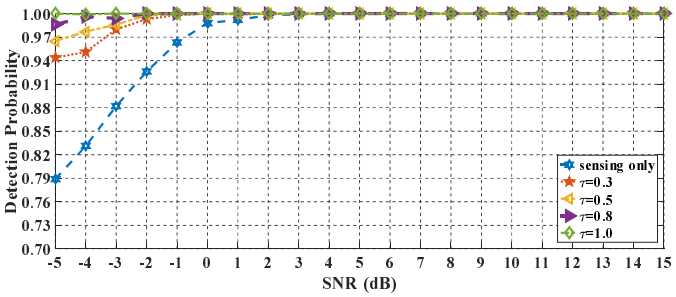

Fig. 10. Detection Probability P_d vs. number of SNR (dB) under different ratio of known part $\tau = 0.3, 0.5, 0.8, 1.0$ and sensing only.

2) Detection Performance with the Prior Information in the Geo-location Database: As the active channel set $\mathcal{S}$ is randomly generated from $\{\mathbb{Z} \cap [1, L]\}$, among which the prior known part $\mathcal{T}$ obtained from geo-location database are randomly chosen from the elements of $\mathcal{S}$. The ratio of the prior known part $\mathcal{T}$ in the active channel set $\mathcal{S}$, referred as τ, is varied between 0 to 1. The case $\tau = 0$ and $\tau = 1$ corresponds to the sensing only case without assists from geo-location database and the case that current channel occupancy states from geo-location database are fully reliable and no change occurs on the spectrum at current time.

Firstly, the received SNR is set as -5 dB and the number of coset samplers p is varied from 15 to 35. As shown in the Fig. 9, the detection performance P_d generally increases with the involved number of coset samplers p, and also improves as the percentage of the known part τ increases. With the input from geo-location database, the number of coset samplers is further reduced in the the proposed joint sensing scheme to achieve the same detection probability compared with the sensing only case. For example, to achieve the desired detection probability of 0.97, sensing only method needs around $p = 20$ coset samplers, while the proposed joint sensing scheme needs only $p = 15$ coset samplers. Moreover, the proposed scheme can update the lack of channel occupancy information in the geo-location database, which helps to improve the detection performance and reduce the required number of coset samplers in the subsequent sensing activities.

Secondly, the detection performance is evaluated with varying received SNR from -5 dB to 15 dB in Fig. 10 with fixing the number of coset sampler as $p = 15$ to sample the received signals. As shown in Fig. 10, the detection performance of the proposed joint sensing scheme utilizing different ratio of known part τ is always superior to that of the sensing only, especially more sensitive to the low SNR region.

3) Detection Performance with the Partially Incorrect Prior Information in the Geo-location Database: Both Fig. 9 and Fig. 10 follow that the prior information from geo-location database is correct for all given channels. As stated in Section IV, it may be the case that the information from geo-location database is not fully reliable, e.g., some of the channel occupancy states are changed but the geo-location database has not been updated timely. In this situation, the proposed joint sensing scheme can still recover the actual signals since it could remove the incorrect elements in $\mathcal{T}$ from the minimization problem, but more cost samplers are adopted compared with the case when no errors are present in $\mathcal{T}$.

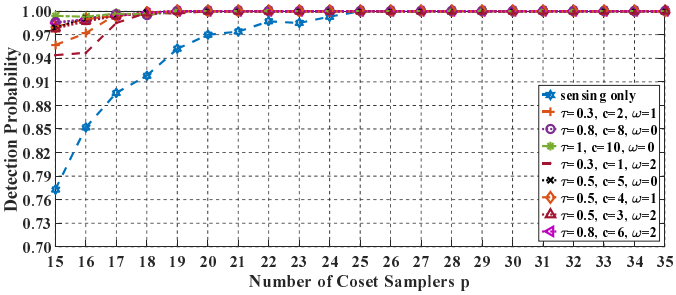

Fig. 11. Detection Probability P_d vs. number of coset samplers p under different ratio of known part with partially incorrect prior information and sensing only.

In Fig. 11, the cases in which $\mathcal{T}$ contains some incorrect prior information are simulated, which means that apart from the c channels correctly belonging to the support, there are ω out of $\tau|\mathcal{S}|$ channels in $\mathcal{T}$ that do not belong to the current signal support. The simulation setting is same as that in Fig. 9 and Fig. 10, but with different combinations of c and ω in $\mathcal{T}$. As shown in the Fig. 11, the proposed scheme can still reconstruct the underlying signals and shows an improvement in detection performance with respect to the case with no prior information.

4) Detection Performance with the Partially Incorrect Prior Information in the Geo-location Database over Real-world Signal: Finally, we apply the proposed scheme on the collected real-world signal to validate the proposed scheme in the practical environment. It is shown in Fig. 12 that the proposed scheme could recover the spectrum even with the partially incorrect prior information from the geo-location database and the detection performance of the proposed joint sensing scheme still is superior to that of the sensing only.

VI. Conclusion

In this paper, we proposed a blind joint sub-Nyquist wideband spectrum sensing scheme for cognitive IoT, which only requires the off-the-shelf low-rate ADCs in the wireless IoT devices which have cognitive capabilities. Without the prior knowledge of the number of occupied channels and the level of SNRs, the proposed scheme could blindly select sufficient number of coset samplers to achieve desired sensing performance. To further reduce the required number of the

This article has been accepted for publication in a future issue of this journal, but has not been fully edited. Content may change prior to final publication. Citation information: DOI 10.1109/JIOT.2018.2837891, IEEE Internet of Things Journal

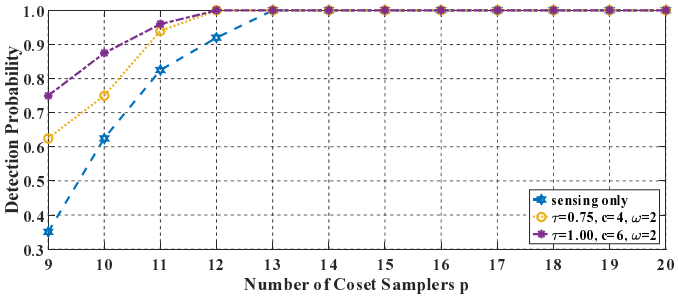

Fig. 12. Detection Probability P_d vs. number of coset samplers p under different ratio of known part with partially incorrect prior information over real-world signals.

coset samplers, the processing complexity and the energy consumption over the evolved IoT devices, we proposed to incorporate the channel occupancy information from the geo-location database and the wideband signal reconstruction process. Moreover, with the awareness that the information from geo-location is not fully reliable, the proposed scheme could reconstruct the signal with partially correct information and return the newly updated information to databases. Experimental results have shown that the proposed scheme could not only utilize the minimum number of coset samplers without known number of occupied channels but also guarantee the desired detection performance under wide range of SNRs. Moreover, the performance of the proposed scheme assisted with geo-location database is superior to the sensing only method even when the obtained information is partially correct, especially in low SNR region. These benefits from the proposed scheme make it be a good candidate for the large-scale deployment of the power constrained IoT devices and spectrum management.

REFERENCES

[1] Y. Gao, Z. Qin, Z. Feng, Q. Zhang, O. Holland, and M. Dohler, "Scalable & reliable IoT enabled by dynamic spectrum management for M2M in LTE-A," *IEEE Internet of Things Journal*, vol. 3, no. 6, pp. 1135 – 1145, May 2016.

[2] A. Aijaz and A. H. Aghvami, "Cognitive machine-to-machine communications for Internet of Things: A protocol stack perspective," *IEEE Internet of Things Journal*, vol. 2, no. 2, pp. 103–112, Jan. 2015.

[3] K. Wang, X. Qi, L. Shu, D.-J. Deng, and J. J. Rodrigues, "Toward trustworthy crowdsourcing in the social internet of things," *IEEE Wireless Commun.*, vol. 23, no. 5, pp. 30–36, Oct. 2016.

[4] K. Wang and Y. Yu, "A query–matching mechanism over out–of–order event stream in IoT," *International Journal of Ad Hoc and Ubiquitous Computing*, vol. 13, no. 3-4, pp. 197–208, May 2013.

[5] P. Rawat, K. D. Singh, and J. M. Bonnin, "Cognitive radio for M2M and Internet of Things: A survey," *Comput. Commun.*, vol. 94, pp. 1–29, Nov. 2016.

[6] Office of Commun. (Jul. 2009). *Digital dividend: cognitive access.* [Online]. Available: http://stakeholders.ofcom.org.uk/binaries/consultations/cognitive/statement/statement.pdf

[7] Agre, Jonathan R. and Gordon, Karen D. (Sept. 2015). *Summary of Recent Federal Government Activities to Promote Spectrum Sharing*. [Online]. Available: https://www.ida.org/idamedia/Corporate/Files/Publications/STPIPubs/2015/p5186final.pdf

[8] M. Fitch, M. Nekovee, S. Kawade, K. Briggs, and R. MacKenzie, "Wireless service provision in TV white space with cognitive radio technology: A telecom operator's perspective and experience," *IEEE Commun. Mag.*, vol. 49, no. 3, Mar. 2011.

[9] Q. Wu, G. Ding, Y. Xu, S. Feng, Z. Du, J. Wang, and K. Long, "Cognitive internet of things: a new paradigm beyond connection," *IEEE Internet of Things Journal*, vol. 1, no. 2, pp. 129–143, Mar. 2014.

[10] J. A. Stankovic, "Research directions for the internet of things," *IEEE Internet of Things Journal*, vol. 1, no. 1, pp. 3–9, Mar. 2014.

[11] K. Wang, Y. Wang, Y. Sun, S. Guo, and J. Wu, "Green industrial internet of things architecture: an energy-efficient perspective," *IEEE Commun. Mag.*, vol. 54, no. 12, pp. 48–54, Dec. 2016.

[12] Y. Ma, X. Zhang, and Y. Gao, "Joint Sub-Nyquist Spectrum Sensing Scheme with Geolocation Database over TV White Space," *IEEE Trans. Veh. Technol.*, Oct. 2017 (To appear).

[13] J. J. Meng, W. Yin, H. Li, E. Hossain, and Z. Han, "Collaborative spectrum sensing from sparse observations in cognitive radio networks," *IEEE J. Sel. Areas Commun.*, vol. 29, no. 2, pp. 327–337, Jan. 2011.

[14] A. Sahai and D. Cabric, "Spectrum sensing: fundamental limits and practical challenges," in *Proc. IEEE Int. Conf. Dyn. Spectr. Access Netw. (DySPAN)*, Baltimore, MD, Dec. 2005.

[15] Y. Pei, Y.-C. Liang, K. C. Teh, and K. H. Li, "Energy-Efficient Design of Sequential Channel Sensing in Cognitive Radio Networks: Optimal Sensing Strategy, Power Allocation, and Sensing Order," *IEEE J. Sel. Areas Commun.*, vol. 29, no. 8, pp. 1648–1659, Sep. 2011.

[16] Z. Qin, Y. Gao, and M. D. Plumbley, "Malicious user detection based on low-rank matrix completion in wideband spectrum sensing," *IEEE Trans. Signal Process.*, vol. 66, no. 1, pp. 5–17, Jan.

[17] D. L. Donoho, "Compressed sensing," *IEEE Trans. Inf. Theory*, vol. 52, no. 4, pp. 1289–1306, Apr. 2006.

[18] Z. Qin, J. Fan, Y. Liu, Y. Gao, and G. Y. Li, "Sparse representation for wireless communications," *IEEE Signal Process. Mag.*, 2018(to appear).

[19] Z. Tian and G. B. Giannakis, "Compressed sensing for wideband cognitive radios," in *Proc. IEEE Int. conf. on Acoust., Speech and Signal Process. (ICASSP)*, Honolulu, HI, Apr. 2007, pp. 1357–1360.

[20] Z. Qin, Y. Gao, M. Plumbley, and C. Parini, "Wideband spectrum sensing on real-time signals at sub-Nyquist sampling rates in single and cooperative multiple nodes," *IEEE Trans. Signal Process.*, vol. 64, no. 12, pp. 3106–3117, Jun. 2016.

[21] J. A. Tropp, J. N. Laska, M. F. Duarte, J. K. Romberg, and R. G. Baraniuk, "Beyond nyquist: Efficient sampling of sparse bandlimited signals," *IEEE Trans. Inf. Theory*, vol. 56, no. 1, pp. 520–544, Jan. 2010.

[22] M. Mishali and Y. C. Eldar, "Blind multiband signal reconstruction: compressed sensing for analog signals," *IEEE Trans. Signal Process.*, vol. 57, no. 3, pp. 993–1009, Mar. 2009.

[23] Y. Ma, Y. Gao, Y.-C. Liang, and S. Cui, "Reliable and efficient sub-Nyquist wideband spectrum sensing in cooperative cognitive radio networks," *IEEE J. Sel. Areas Commun.*, vol. 34, no. 10, pp. 2750–2762, Oct. 2016.

[24] T. Xiong, H. Li, P. Qi, Z. Li, and S. Zheng, "Pre-decision for wideband spectrum sensing with sub-Nyquist sampling," *IEEE Trans. Veh. Technol.*, vol. PP, no. 99, pp. 1–1, Jan. 2017.

[25] M. R. Palattella, M. Dohler, A. Grieco, G. Rizzo, J. Torsner, T. Engel, and L. Ladid, "Internet of things in the 5G era: Enablers, architecture, and business models," *IEEE J. Sel. Areas Commun.*, vol. 34, no. 3, pp. 510–527, Feb. 2016.

[26] Z. Qin, Y. Gao, and C. G. Parini, "Data-assisted low complexity compressive spectrum sensing on real-time signals under sub-Nyquist rate," *IEEE Trans. Wireless Commun.*, vol. 15, no. 2, pp. 1174–1185, Feb. 2016.

[27] Z. Quan, S. Cui, A. H. Sayed, and H. V. Poor, "Optimal multiband joint detection for spectrum sensing in cognitive radio networks," *IEEE Trans. Signal Process.*, vol. 57, no. 3, pp. 1128–1140, Mar. 2009.

[28] T. Yucek and H. Arslan, "A survey of spectrum sensing algorithms for cognitive radio applications," *IEEE Commun. Surveys Tutorials*, vol. 11, no. 1, pp. 116–130, Jan. 2009.

[29] Y.-C. Liang, Y. Zeng, E. C. Y. Peh, and A. T. Hoang, "Sensing-throughput tradeoff for cognitive radio networks," *IEEE Trans. Wireless Commun.*, vol. 7, no. 4, pp. 1326–1337, Apr. 2008.

[30] W. Zhang, R. K. Mallik, and K. B. Letaief, "Optimization of cooperative spectrum sensing with energy detection in cognitive radio networks," *IEEE Trans. Wireless Commun.*, vol. 8, no. 12, pp. 5761–5766, Dec. 2009.

[31] C. J. Miosso, R. von Borries, and J. Pierluissi, "Compressive sensing with prior information: Requirements and probabilities of reconstruction in l_0-minimization," *IEEE Trans. Signal Process.*, vol. 61, no. 9, pp. 2150–2164, May 2013.

[32] N. Vaswani and W. Lu, "Modified-CS: Modifying compressive sensing for problems with partially known support," *IEEE Trans. Signal Process.*, vol. 58, no. 9, pp. 4595–4607, Feb. 2010.

[33] P. Feng and Y. Bresler, "Spectrum-blind minimum-rate sampling and reconstruction of multiband signals," in *Proc. IEEE Int. conf. on Acoust.,*

Speech and Signal Process. (ICASSP), vol. 3, Atlanta, GA, May 1996, pp. 1688–1691.

[34] J. Matoušek, "On variants of the johnson-lindenstrauss lemma," *Random Struct. & Algorithms*, vol. 33, no. 2, pp. 142–156, Sep. 2008.

[35] B. Nielson and D. R. Cox, *Asymptotic Techniques for Use in Statistics*, 1st ed. London; New York: Chapman and Hall/CRC, 1989.

[36] J. Chen and X. Huo, "Theoretical Results on Sparse Representations of Multiple-Measurement Vectors," *IEEE Trans. Signal Process.*, vol. 54, no. 12, pp. 4634–4643, Dec. 2006.

[37] J. A. Tropp, A. C. Gilbert, and M. J. Strauss, "Simultaneous sparse approximation via greedy pursuit," in *Proc. IEEE Int. conf. on Acoust., Speech and Signal Process. (ICASSP)*, Philadelphia, PA, Mar. 2005.

[38] J. A. Tropp and A. C. Gilbert, "Signal Recovery From Random Measurements Via Orthogonal Matching Pursuit," *IEEE Trans. Inf. Theory*, vol. 53, no. 12, pp. 4655–4666, Dec. 2007.

[39] J. F. Determe, J. Louveaux, L. Jacques, and F. Horlin, "On the exact recovery condition of simultaneous orthogonal matching pursuit," *IEEE Signal Process. Lett.*, vol. 23, no. 1, pp. 164–168, Jan. 2016.

[40] M. Wang, W. Xu, and A. Tang, "On the performance of sparse recovery via l_p-minimization," *IEEE Trans. Inf. Theory*, vol. 57, no. 11, pp. 7255–7278, Nov. 2011.

[41] X. Zhang, Y. Ma, Y. Gao, and S. Cui, "Real-time adaptively-regularized compressive sensing in cognitive radio networks," *IEEE Trans. Veh. Technol.*, vol. PP, no. 99, pp. 1–1, 2017.

[42] F. Cao, M. Cai, Y. Tan, and J. Zhao, "Image super-resolution via adaptive l_p $(0 < p < 1)$ regularization and sparse representation," *IEEE Trans. on Neural Networks. and Learning Syst.*, vol. 27, no. 7, pp. 1550–1561, Jul. 2016.

[43] X. Zhang, Y. Zhang, Y. Ma, and Y. Gao, "RealSense: Real-time compressive spectrum sensing testbed over TV white space," in *Proc. IEEE Int. conf. on World of Wireless, Mobile and Multimedia Netw. (WoWMoM)*, Macau, China, Jun. 2017.

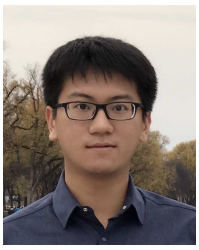

Xingjian Zhang (S'16) received the B.Sc. degree (First Class Hons.) in telecommunications engineering from Beijing University of Posts and Telecommunications, Beijing, China. He is currently working towards his Ph.D. degree in the School of Electronic Engineering and Computer Science, Queen Mary University of London since 2014. His current research interests include cooperative wireless sensor networks, compressive sensing, real-time spectrum monitoring and analysis, and Internet of things (IoT) applications.

Yuan Ma (S'15-M'17) received the B.Sc. degree (First Class Hons.) in telecommunications engineering from Beijing University of Posts and Telecommunications, Beijing, China, and the Ph.D. degree in electronic engineering from Queen Mary University of London, London, U.K., in 2013 and 2017, respectively. She is currently an Assistant Professor with the College of Information Engineering, Shenzhen University, Shenzhen, China. Her research interests include cognitive and cooperative wireless networking, sub-Nyquist signal processing, and spectrum analysis, detection, and sharing over TV white space.

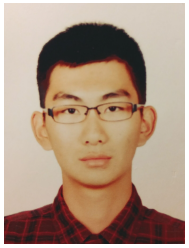

Haoran Qi (S'16) received the B.Eng. degree from Beihang University, China and M.Eng. with first class from The University of Nottingham, U.K. in 2016. He is currently pursuing the Ph.D. degree with the Department of Electronic Engineering and Computer Science in Queen Mary University of London, U.K. His research interests include spectrum sensing, cooperative cognitive radio networks, and sub-Nyquist signal processing.

Yue Gao (S'03-M'07-SM'13) is a Reader in Antennas and Signal Processing, and Director of Whitespace Machine Communication Lab in the School of Electronic Engineering and Computer Science at Queen Mary University of London (QMUL) in the UK. He worked as Research Assistant, Lecturer and Senior Lecturer at QMUL after having received his PhD degree from QMUL in 2007. He is currently leading a team developing theoretical research into practice in the interdisciplinary area among smart antennas, signal processing, spectrum sharing and internet of things (IoT) applications. He has published over 140 peer-reviewed journal and conference papers, 2 patents, and 2 book chapters. He is a co-recipient of the EU Horizon Prize Award on Collaborative Spectrum Sharing in 2016, and Research Performance Award from Faulty of Science and Engineering at QMUL in 2017. He is an Engineering and Physical Sciences Research Council (EPSRC) Fellow from 2018 - 2023.

He is an Editor for the IEEE Transactions on Vehicular Technology, IEEE Wireless Communication Letter and China Communications. He is serving as Cognitive Radio Symposium Co-Chair of the IEEE GLOBECOM 2017. He served as the Signal Processing for Communications Symposium Co-Chair for IEEE ICCC 2016, Publicity Co-Chair for IEEE GLOBECOM 2016, and General Chair of the IEEE WoWMoM and iWEM 2017. He is a Senior Member of IEEE, a Secretary of the IEEE Technical Committee on Cognitive Networks, and an IEEE Distinguished Lecturer of Vehicular Technology Society.

Zhixun Xie is a Deputy Director at the Guangxi Veterinary Research Institute(GVRI), and Guangxi Key Laboratory of Veterinary Biotechnology (GKLVB), in the Guangxi, China. He works as Assistant Professor, Associate Professor and Professor at GVRI and GKLVB after has received DVM in 1984. He had worked for three years as a visiting scientist in the Southeast Poultry Research Laboratory, Department of Agriculture, and the University of Connecticut in the USA. He is a National Ten-Thousand Talents Program of China in 2016 and national candidate of Talents of the New Century in 2006, and was awarded special allowances issued by the Chinese State Department in 1999. He has also been honored by various kinds of research awards, such as National Outstanding Returned Overseas Scholar, Guangxi Distinguished Expert, and Guangxi Advanced Worker for his outstanding contribution in the animal disease research activities.

He has published 483 scientific research papers in peer-reviewed national and international journals, including more than 60 publications in SCI journals, 3 monographs, as well as 69 authorized patents including one USA patent and one national new drug certificate.

Zhiqin Xie is a Professor at Guangxi Veterinary Research Institute (GVI) since 2010. He currently works in the research team which prevents and control animal diseases in GVI. He has worked on 10 research projects, which were funded by Ministry of Science and Technology of China and Guangxi Provincial grants. He currently works on Sino-British Innovation Bridge Project about spectrum sharing and Internet of Things (IoT). He has published over 260 papers, 6 patents, and 1 book chapter.

Minxiu Zhang currently works as a Research Assistant at Guangxi Veterinary Research Institute (GVI) in China after having received her Master's degree in Veterinary Medicine from Guangxi University in 2012. She is currently engaging in research technology and animal etiology. She has published 12 journal papers and 1 patent.

Xiaodong Wang is the founder and CEO of Guangxi TalentCloud Information Technology Co., Ltd. He graduated from Peking University and Hong Kong Polytechnic University. He worked for Microsoft as Senior Manager from 2005 to 2009. Because of the contribution to Windows 7 Launch, he won Microsoft Chairman Award in 2009. In 2012, He founded TalentCloud which focuses on Agriculture IoT and AI research. Till now, TalentCloud cloud-based smart agriculture platform has served more than 1000 farms all over China.

Guangliang Wei is the CTO of Guangxi TalentCloud Information Technology Co., Ltd. He has experience in software development and management over 15 years. From 2004 to 2008, he worked as the member of the Kingdee "K/3 HR" founding team regarding the product design and development. From 2009 to 2011, he served as the core architect of the new generation of ERP products (K/3 Cloud). He is currently leading a team developing theoretical research into practice in the interdisciplinary areas of AI and IoT applications. He has published over 5 papers, 16 patents.

Zheng Li is an engineer of Guangxi TalentCloud Information Technology Co., Ltd. He has rich experience in hardware research and development over 10 years. He is currently working on developing theoretical research into practice in the application of IoT. He has published over 5 papers and 7 patents.